

A buffer zone in the crystal structure that governs the solid-state photodimerization of bulky olefins with the 1,4-dihydropyridine skeleton



Nobuhiro Marubayashi,^{*,a} Takayuki Ogawa,^a Toshio Hamasaki^a and Noriaki Hirayama^b

^a Research Laboratories, Yoshitomi Pharmaceutical Industries Ltd., 955 Koikai, Yoshitomi-cho, Chikugo-gun, Fukuoka 871, Japan

^b Department of Biological Science and Technology, Tokai University, 317 Nishino, Numazu, Shizuoka 410-03, Japan

Due to steric hindrance, bulky olefins cannot readily undergo solid-state photodimerization. UV irradiation of crystals of (4*RS*,1'*RS*)-methyl 1-phenyl-2-piperidinoethyl 1,4-dihydro-2,6-dimethyl-4-(2-thienyl)pyridine-3,5-dicarboxylate (**1**), however, affords a single product (4*RS*,8*SR*)-4*a*,8*a*-dimethoxycarbonyl-2,4*b*,6,8*b*-tetramethyl-3-[(1*RS*)-1-phenyl-2-piperidinoethoxycarbonyl]-7-[(1*SR*)-1-phenyl-2-piperidinoethoxycarbonyl]-4,8-di(2-thienyl)-1,4,4*a*,4*b*,5,8,8*a*,8*b*-octahydro-*trans*-cyclobuta-[1,2-*b*:3,4-*b'*]dipyridine (**2**), in quantitative yield. X-Ray analyses of **1** and **2** showed that **2** is a photodimer of **1** and proved that bulky olefins can undergo solid-state photodimerization. Although the molecular system and the molecular arrangement in the crystal of dimethyl 1,4-dihydro-2,6-dimethyl-4-(3-nitrophenyl)pyridine-3,5-dicarboxylate (**3**) are quite similar to those of **1**, crystals of **3** cannot undergo solid-state photodimerization. Detailed inspection of the crystal structure of **1** revealed that there is a certain space between reacting molecules in the crystal to allow initiation of photodimerization. The space, designated as a buffer zone, buffers the steric hindrance from which the reacting molecules suffer when they approach each other. The buffer zone is formed by the disordered piperidine rings in **1**, but there is no extra space in the crystal structure of **3**. The present study has shown that the buffer zone in the crystal structure must be one of the prerequisite controlling factors for solid-state photodimerization.

Introduction

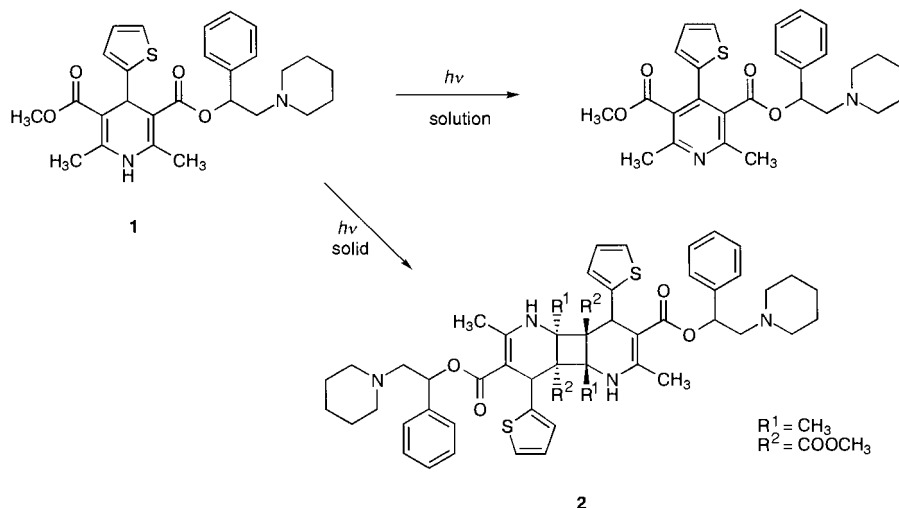
Solid-state photodimerization of olefins is one of the well-known topochemical photoreactions.¹ For the interpretation of the mechanisms of photodimerization, the relationships between the packing of molecules in the crystal and reactivity are very important because such reactions proceed under the strict control of the crystal lattice. Schmidt and his co-workers established the first topochemical rule based on systematic studies on the photodimerization of cinnamic acid derivatives.² According to this rule, reactions in crystals proceed with minimal atomic and molecular movement, and photodimerization is solely the result of a packing arrangement that orientates the reacting double bonds in parallel with the centre-to-centre distance at 4.2 Å or less. Since Schmidt's pioneering work however, some examples which significantly deviate from the topochemical rule have also been reported.^{1,3} In these structures solid-state photodimerization does not occur in spite of favourable crystal packing. Some of these exceptions were explained in terms of Cohen's 'reaction cavity' principle,⁴ an extension of the topochemical rule. The principle states that solid-state reactions proceed with minimal change or distortion of the reaction cavity formed by the molecules surrounding the transition state of the reaction complex in the crystal. More recently, Gavezzotti generalized that a prerequisite for crystal reactivity is the availability of free space around the reaction site.⁵

On the basis of these principles, it seems quite reasonable that bulky olefins do not undergo photodimerization even though the arrangement of reactive double bonds satisfies the geometrical prerequisite (Schmidt's rule) because mobility of molecules must be highly restricted in the crystal. It is of interest to know whether or not bulky olefins can photodimerize in the crystal. No systematic studies on photodimerization of bulky olefinic systems, however, have been made so far. Since

many 1,4-dihydropyridines have been synthesized as biologically important calcium channel antagonists, we planned to investigate photodimerization of 4-aryl-1,4-dihydropyridines as an example of bulky olefinic systems. We found that irradiation of (4*RS*,1'*RS*)-methyl 1-phenyl-2-piperidinoethyl 1,4-dihydro-2,6-dimethyl-4-(2-thienyl)pyridine-3,5-dicarboxylate (**1**) in the solid state can actually give a photodimer **2** in quantitative yield in spite of the presence of bulky groups as shown in Scheme 1. In this paper, we present the results of photochemical and crystallographic studies on **1** and the related compounds towards understanding the mechanism of photodimerization of the bulky olefinic system.

Results and discussion

In the course of development of calcium channel antagonists, compound **1** was synthesized.⁶ Irradiation by UV light of a methanol solution of **1** (0.1%) for 24 h resulted in formation of a trace amount of the pyridine derivative (Scheme 1). This result is reasonably expected from the well-known photodecomposition of 1,4-dihydropyridines.⁷ Photolysis of the crystal of **1**, however, proceeds rapidly and quantitatively to give a single product (**2**) without formation of the pyridine derivative. The result seems to indicate that **1** undergoes a topochemical photoreaction in the solid state. To confirm the structure of **2**, the X-ray analysis of the perchlorate salt of **2** was undertaken. As shown in Fig. 1, it was proved that **1** gives the photodimerization product **2**. The structure of **2** has a crystallographic centre of inversion. Selected geometrical parameters are listed in Table 1, where they are compared with those of **1** and **3** (see below). The diazatricyclododecadiene moiety adopts the *syn-syn* conformation, and the tetrahydropyridine ring adopts a slightly twisted boat conformation with the 4-thienyl ring in a pseudoaxial orientation. The bond distance of the cyclobutane



Scheme 1

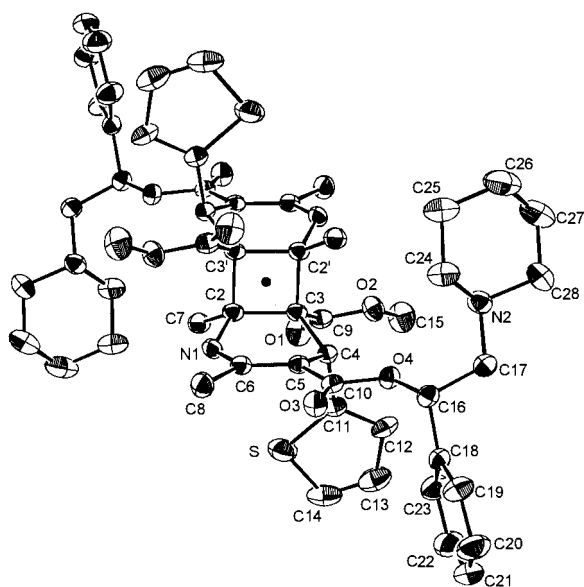


Fig. 1 ORTEP drawing of the structure of **2** showing the 40% probability ellipsoids. Perchlorate anions and solvate molecules are omitted for clarity.

ring connecting the two half molecules is long [1.609(5) Å] presumably due to the steric hindrance between the bulky substituents attached to the cyclobutane ring.

According to Schmidt's topochemical rule, the reactive double bonds for photodimerization should be close (*ca.* 4 Å) and nearly parallel in the crystal structure.² Therefore, in the crystal structure of **1**, the relevant double bonds should take the orientation that satisfies Schmidt's rule. X-Ray analysis of **1** was performed to understand the susceptibility of the topochemical reaction and to obtain the precise geometrical parameters of the crystal structure of the starting material. The molecular structure of **1** is depicted in Fig. 2 as a pair related by a crystallographic centre of symmetry. Selected geometrical parameters of **1** are listed in Table 1. The dihydropyridine moiety adopts the typical conformation of the 4-aryl-1,4-dihydropyridines,⁸ *i.e.* a flat-boat conformation with the 4-aryl substituent in a pseudoaxial orientation. The geometrical parameters describing the relative orientation of two double bonds in the crystal are defined in Scheme 2 and listed in Table 2. The reacting double bonds in the dihydropyridine rings related by the centre of symmetry are parallel with a centre-to-centre distance (D_1) of 3.728(6) Å and a slight displacement (D_2) of 0.14(1) Å. The data demonstrate that the molecules in the crystal structure of **1** can be highly photoreactive and could

Table 1 Selected bond distances, bond angles and torsion angles for **2**, **1** and **3**

	2	1	3
Bond distances/Å			
N1–C2	1.466(3)	1.384(6)	1.383(2)
N1–C6	1.362(3)	1.379(6)	1.381(2)
C2–C3	1.561(4)	1.337(6)	1.346(2)
C3–C4	1.565(4)	1.520(6)	1.517(2)
C4–C5	1.522(3)	1.521(6)	1.518(2)
C5–C6	1.365(4)	1.360(6)	1.352(2)
C2–C3'	1.609(5)	3.728(6) ^a	3.725(3) ^a
Bond angles (°)			
C2–N1–C6	126.3(3)	123.4(4)	123.5(1)
N1–C2–C3	111.8(2)	118.9(4)	118.7(1)
C2–C3–C4	115.4(2)	121.0(4)	120.7(1)
C3–C4–C5	113.2(2)	111.1(3)	110.8(1)
C4–C5–C6	118.7(2)	119.2(4)	120.5(1)
N1–C6–C5	119.5(2)	119.5(4)	118.7(1)
C3–C2–C3'	89.5(2)	87.8(3) ^a	92.4(1) ^a
C2–C3–C2'	90.5(2)	92.2(3) ^a	87.6(1) ^a
Torsion angles (°)			
C6–N1–C2–C3	–25.8(4)	–15.1(6)	–15.4(3)
C2–N1–C6–C5	24.8(4)	12.1(6)	15.2(3)
N1–C2–C3–C4	–5.3(3)	–4.8(6)	–6.6(3)
C2–C3–C4–C5	33.6(3)	24.0(5)	25.2(2)
C3–C4–C5–C6	–37.6(4)	–26.6(5)	–25.4(2)
C4–C5–C6–N1	10.0(4)	10.4(6)	7.1(2)

^a Non-bonded distances and angles.

afford the centrosymmetric photodimer **2**. It should be noted that the piperidine ring is disordered over two sites in the crystal and the ring adopts two conformations which are populated at 70 and 30%, respectively. The major conformation is a chair form with the adjacent methylene group of equatorial orientation. The minor one is a flattened chair form with the methylene group of pseudoaxial orientation.

The molecular packing of **1** is shown in Fig. 3. There are two distinct interfaces between molecules in the crystal. One interface is between dihydropyridine moieties and the other between thienyl and phenyl rings. The former interfaces include weak intermolecular hydrogen bonds between the dihydropyridine N–H and the ester C=O [N...O 2.980(5) Å]. The hydrogen bonds may have an important role in bringing the two centrosymmetrically related molecules close together. The latter interfaces are formed by the hydrophobic interactions. As shown in Fig. 3, the disordered piperidine rings are located in these interfaces. It is considered that the disordered region where the piperidine rings adopt the two conformations are formed

as a result of the crystal packing by hydrophobic interactions between the aromatic rings.

The superposition of the molecular structures of **1** and **2** is shown in Fig. 4 to illustrate the comparison between the structures before and after photoreaction. The molecular shape of the dimer as a whole is similar to that of the two centrosym-

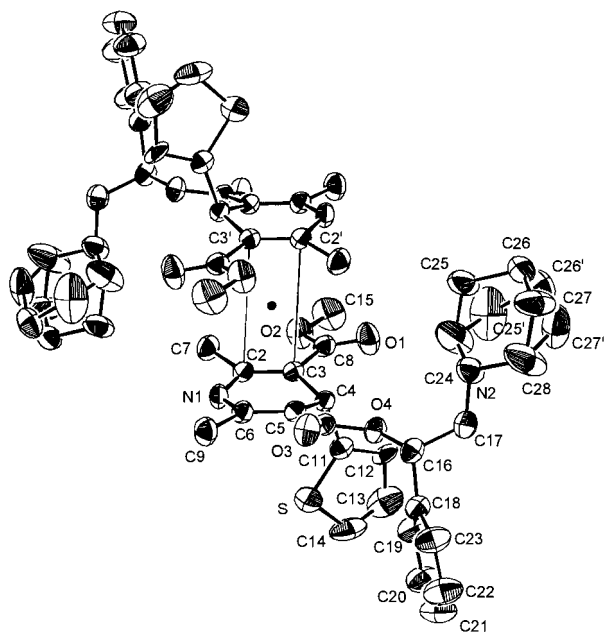
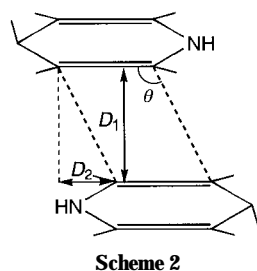


Fig. 2 ORTEP drawing of two centrally related molecules of **1** showing the 40% probability ellipsoids. Thin lines represent the routes for photodimerization.



Scheme 2

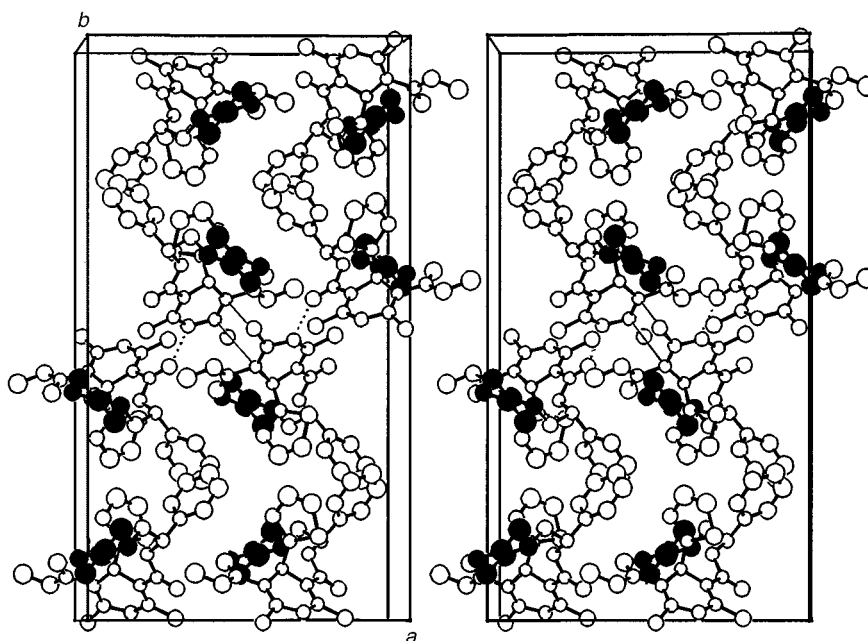


Fig. 3 Packing diagram of **1** viewed down the c axis. To avoid congestion, only major conformers of the piperidine ring are shown (black sphere). Thin lines represent the routes for photodimerization and dotted lines represent intermolecular hydrogen bonds.

metrically related monomers. Most atoms in the monomer are translationally shifted towards the centre of the dimer. According to Schmidt's topochemical rule, reactions in crystals will proceed with minimal atomic and molecular movement. In the case of the photodimerization of **1** to **2**, however, not only atoms near the reacting double bond but also peripheral atoms seem to have moved more than 0.5 Å.

Many 4-aryl-1,4-dihydropyridines have been synthesized and their chemical behaviour has been well studied, but their photodimerization has never been reported. The literature on the crystal structures of molecules with the 1,4-dihydropyridine skeleton in the Cambridge Structural Database⁹ was thoroughly surveyed in order to analyse intermolecular interactions between the dihydropyridine rings in the crystal. It was found that a few compounds form crystal structures that can be considered to be highly photoreactive on the basis of Schmidt's rule alone. In particular, in the crystal structure of dimethyl 1,4-dihydro-2,6-dimethyl-4-(3-nitrophenyl)pyridine-3,5-dicarboxylate (**3**, Scheme 3),^{8b} the relative orientation of the double bonds is almost equivalent to that of **1**. All geometrical parameters for **3**, however, have not been published yet and the final R value in the literature is relatively high ($R = 0.107$).^{8b} Therefore, we have recrystallized compound **3** and undertaken the X-ray analysis again. The molecular structure of **3** related by a crystallographic centre of symmetry is depicted in Fig. 5. Selected geometrical parameters of **3** are listed in Table 1. As indicated in Fig. 5 and Table 2, the crystal of **3** must be photoreactive according to Schmidt's rule. However, UV irradiation of crystals of **3** under the same conditions as photolysis of **1** (48 h) resulted in 99% recovery of the starting material **3** and formation of a trace amount of the pyridine derivative.

In the crystal structure of **3** (Fig. 6), two interfaces between the molecules are observed; one consists of dihydropyridine

Table 2 Relative orientations of the double bonds for **1** and **3**

	$D_1^a/\text{Å}$	$D_2^b/\text{Å}$	θ^c (°)
1	3.728(6)	0.14(1)	87.8(3)
3	3.725(3)	0.16(1)	92.4(1)
Ideal value ^d	<4.2	0.0	90.0

^a D_1 : centre-to-centre distance between double bonds. ^b D_2 : displacement of double bonds along the double-bond axis. ^c θ : angle of parallelogram formed by double bonds. ^d Schmidt's rule.

moieties and another of nitrophenyl rings. They are similar to those observed in the crystal of **1**. A weak intermolecular hydrogen bond between the dihydropyridine N-H and the ester C=O [$N \cdots O$ 3.048(2) Å] was also observed in the crystal of **3**. In this crystal, however, no part of the molecule is disordered.

The molecular systems of **1** and **3** are quite similar and the geometrical parameters in Table 1 indicate that intramolecular electronic effects may not be crucial in causing the difference in reactivity. As **1** and **3** possess bulky substituents around the reactive bonds, the photodimerization in the crystal seems to be an unlikely event even though they satisfy Schmidt's rule, *i.e.* each atom of the two facing bulky molecules has to move more than 0.5 Å towards the centre of symmetry. Ariel *et al.*^{3a} reported that a bulky olefin lacks solid-state photoreactivity in spite of its ideal molecular arrangement in the crystal from the viewpoint of Schmidt's rule. They attribute the lack of reactivity to the steric hindrance of the bulky substituents.

Although **1** has bulkier substituents than **3**, compound **3** is not photoreactive. These results indicate that proximity and orientation of the reactants in the crystal may be important for photodimerization of 1,4-dihydropyridines but there must also be additional essential factors which promote the reaction in the crystalline state. In the photoreactive crystal structure of **1**, the piperidine rings are disordered over two sites. In the dis-

ordered regions the piperidine rings can adopt two conformations; the van der Waals volume of the whole disordered molecule of **1** is 424.4 Å³ whereas each conformer of **1** occupies only 405.3 and 408.0 Å³, respectively. This means that the space which corresponds to at least 16.4–19.1 Å³ in van der Waals volume is available for the piperidine ring to change its conformation in the crystal. This extra space is not necessary for close packing but useful for the conformational disorder.

In order to inspect the environment around the disordered piperidine rings the crystal structure of **1** and the dimer molecule **2** were superimposed as shown in Fig. 7(a). The dimer molecule can be placed in the crystal structure of **1** without any short contacts with the surrounding molecules except for the piperidine moiety. If the piperidine ring adopts only the major conformation, the distance between the piperidine ring of the dimer and the methyl group of the neighbouring monomer is quite short (the distance between C26 of the dimer and C7 of the neighbouring monomer is 2.40 Å) and it suggests that photodimerization cannot proceed. The major conformer must change its conformation to relieve the steric hindrance. Inspection of the model shows that the extra space in the disordered region in the crystal of **1** can accommodate this conformational change and buffer the steric hindrance caused by approaching

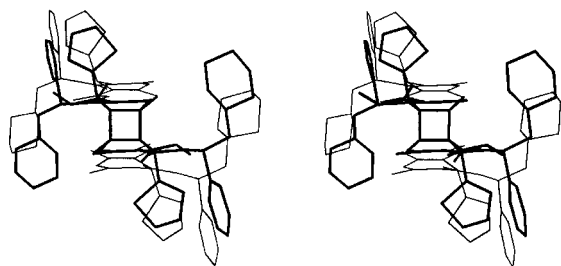
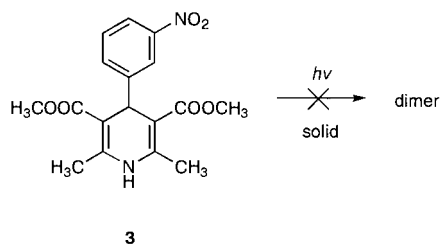


Fig. 4 Superimposition of the X-ray structures of **1** (thin lines; only the major conformation is shown) and **2** (thick lines)



Scheme 3

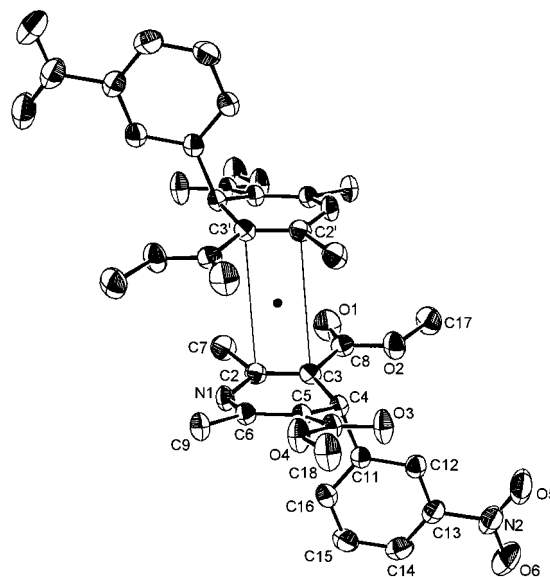


Fig. 5 ORTEP drawing of two centrally related molecules of **3** showing the 40% probability ellipsoids. Thin lines represent the possible routes for photodimerization.

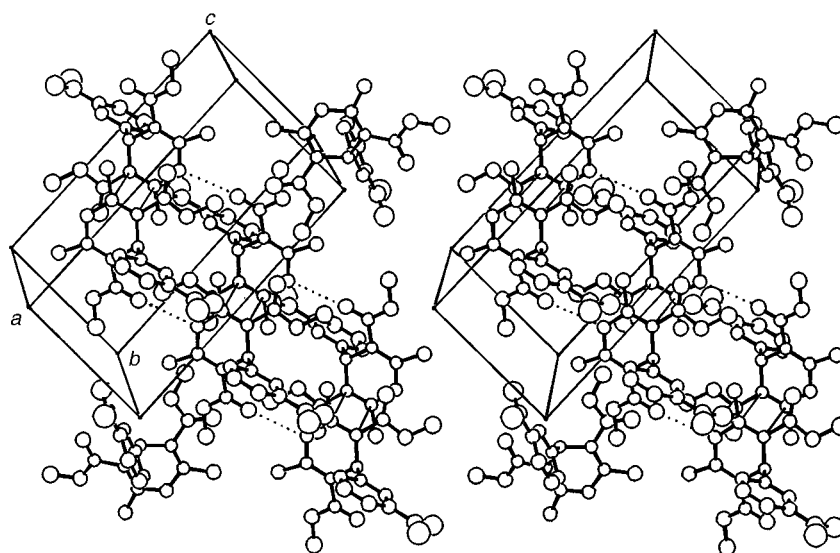


Fig. 6 Packing diagram of **3**. Thin lines represent possible routes for photodimerization and dotted lines represent intermolecular hydrogen bonds.

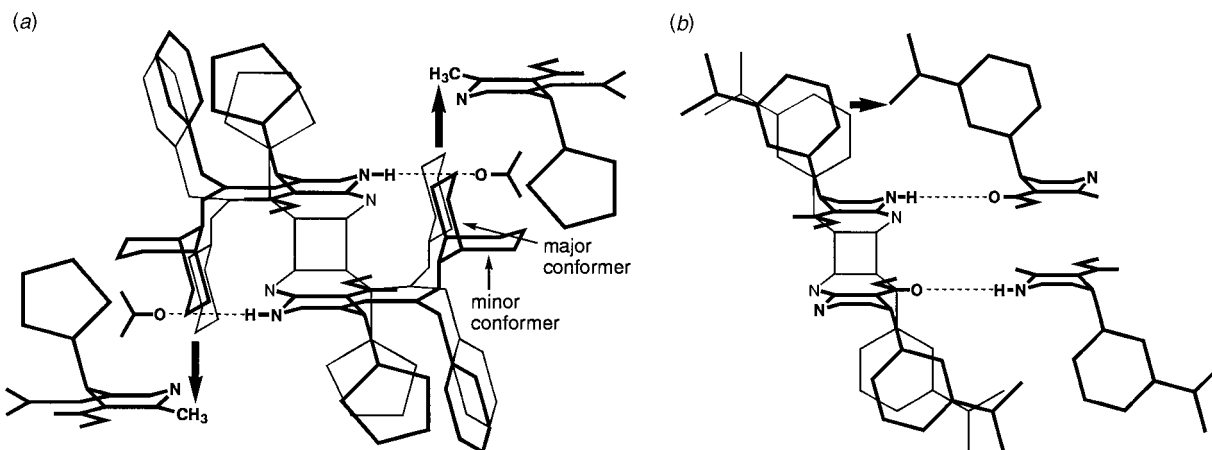


Fig. 7 Schematic drawings of molecular arrangements near the reaction sites in the crystals of **1** (a) and **3** (b). Thick and thin lines represent monomer and dimer molecules, respectively, and dashed lines represent intermolecular hydrogen bonds.

molecules. As the steric hindrance is buffered in the extra space, the space can be designated as a 'buffer zone'. Although the phenylpiperidinoethyl group is intrinsically bulky, it also contains a moiety with conformational flexibility and which contributes to form the buffer zone in the crystal to undergo solid-state photodimerization.

The photostable crystal structure of **3** and its dimer molecule, which was modelled, were also superimposed as shown in Fig. 7(b). In this case, the distance between the nitrophenyl rings of the dimer and the nitro group of the adjacent monomer is quite short (the distance between C15 of the dimer and O5 of the neighbouring monomer is 2.4 Å) although the remaining part of the dimer molecule can be located in the crystal structure of **3** without any short contacts with the surrounding monomer molecules. In the crystal structure of **3**, there is no extra space for conformational changes and it is considered that the close packing of **3** prevents the movement of reactants for dimerization. The compact packing of **3** was also evident from the significantly higher crystal density (1.38 g cm^{-3}) than that of **1** (1.25 g cm^{-3}).

The present study indicates that Schmidt's rule is not sufficient to predict the photodimerization reactivity of bulky olefins from the crystal structures. We propose here that there are at least two factors which control the photodimerization of bulky olefins in the solid state. The first one is the geometrical prerequisite governed by Schmidt's rule. The second one is the buffer zone that maintains the crystal structure in the monomer state and allows the monomer molecules to approach each other to dimerize using the buffer action of this zone. Since the role of the buffer zone is to buffer the intermolecular hindrance and help the reaction sites come close together, the buffer zone is not necessarily located near the reaction sites. The buffer zone located distant from the reaction sites can promote the photodimerization just as in the case of **1**. The concept of the buffer zone is distinct from others described in the introduction so far. A more flexible moiety is more useful as the buffer zone if it can be incorporated in the crystal structure. The idea of the buffer zone would greatly assist us in the molecular design of crystalline photoreactive compounds.

In summary, we have studied the relationships between the crystal structures and reactivity for the solid-state photodimerization of two 1,4-dihydropyridines with bulky substituents, compounds **1** and **3**. X-Ray analyses revealed that both compounds have the same geometrical characteristics of the crystal structure that should be highly susceptible to photodimerization according to Schmidt's rule. Although irradiation of **1** in the crystalline state affords the photodimer **2**, compound **3** in the crystal has been shown to be photostable. The detailed comparison of the crystal structures of **1** and **3** has revealed that one of the bulky substituents forms a disordered zone in the photoreactive crystal of **1**. The disordered substituents consti-

tute the buffer zone that helps molecules to approach in the crystal. The present study has unambiguously pointed out that, in addition to Schmidt's geometrical requirements, the buffer zone in the crystal is essential for the solid-state photodimerization of bulky olefins.

Experimental

(4*RS*,1'*RS*)-Methyl 1-phenyl-2-piperidinoethyl 1,4-dihydro-2,6-dimethyl-4-(2-thienyl)pyridine-3,5-dicarboxylate (**1**) and dimethyl 1,4-dihydro-2,6-dimethyl-4-(3-nitrophenyl)pyridine-3,5-dicarboxylate (**3**) were synthesized at Yoshitomi Pharmaceutical Industries Ltd. (Japan). Spectral measurements were carried out using the following equipment: Hitachi 320 (UV), JEOL GSX400 (^1H and ^{13}C NMR) and JEOL DX300 (mass spectrum). Elemental analysis was performed on a YANACO MT-3 CHN recorder. HPLC analyses were carried out using a Shimadzu LC10AD pump equipped with a Shimadzu SPD6A UV detector and a C-R6A data processor, and conditions were as follows: column, Shimadzu STR ODS-II 4.6 mm i.d. \times 150 mm; mobile phase, 0.05 M perchlorate buffer (pH 2.5)-acetonitrile (1 : 1); flow rate, 1.0 ml min^{-1} ; detection, UV at 263 nm.

Photolyses

Photolyses were performed at room temperature using a Nagano Science LT-120 irradiator equipped with a Toshiba chemical lamp FIR-20S-BL/M ($800 \mu\text{W cm}^{-2}$). The crystalline samples were packed between two glass plates and placed in the irradiator. The time course of the reaction was checked by HPLC periodically. Irradiation of **1** for 3 h afforded the photoproduct **2** in 100% yield. The pyridine derivatives of **1** and **3** were identified by means of HPLC analyses using photodiode array detection by comparison of the retention time and the UV spectra to those of the authentic samples.

Photoproduct 2. White powder, mp 257–258 °C (from MeOH-chloroform) (Found: C, 67.22; H, 6.69; N, 5.79. $\text{C}_{54}\text{H}_{64}\text{N}_4\text{O}_8\text{S}_2$ requires C, 67.47; H, 6.71; N, 5.83%); $\lambda_{\text{max}}/\text{nm}$ (MeOH) 300 ($\epsilon = 34\,070 \text{ dm}^3 \text{ mol}^{-1} \text{ cm}^{-1}$) and 240 ($\epsilon = 19\,840 \text{ dm}^3 \text{ mol}^{-1} \text{ cm}^{-1}$); $\delta_{\text{H}}[400 \text{ MHz}, (\text{CD}_3)_2\text{SO}-\text{CF}_3\text{COOD}$ (95 : 5), 100 °C] 7.20 (3H, m), 7.14 (1H, dd), 7.06 (2H, m), 6.77 (2H, m), 6.66 (1H, s), 6.12 (1H, dd), 4.61 (1H, s), 3.53 (1H, dd), 3.37 (3H, s), 3.32 (1H, dd), 3.22 (4H, m), 2.12 (3H, s), 1.77 (4H, m), 1.71 (3H, s) and 1.56 (2H, m); $\delta_{\text{C}}[100 \text{ MHz}, (\text{CD}_3)_2\text{SO}-\text{CF}_3\text{COOD}$ (95 : 5), 100 °C] 168.63, 164.18, 154.70, 145.87, 138.07, 127.71, 127.33, 125.49, 125.41, 124.60, 123.59, 99.46, 69.48, 66.96, 60.57; 60.14, 53.01, 50.19, 38.61, 22.09, 20.70, 20.40, 20.32 and 17.99; m/z 961 ($[\text{M} + 1]^+$, 20%, FAB).

Single-crystal X-ray analyses

Single crystals of a perchlorate salt of **2** (hereafter simply designated as **2**) were obtained from 0.05 M perchlorate buffer (pH

Table 3 Crystallographic data for **2**, **1** and **3**

	2	1	3
Formula	C ₅₄ H ₆₄ N ₄ O ₈ S ₂ ·2HClO ₄ ·2H ₂ O·2CH ₃ CN	C ₂₇ H ₃₂ N ₂ O ₄ S	C ₁₇ H ₁₈ N ₂ O ₆
Formula mass	1280.30	480.62	346.34
Colour, habit	Colourless, plate	Colourless, plate	Colourless, plate
Size (mm)	0.5 × 0.4 × 0.2	0.3 × 0.3 × 0.1	0.4 × 0.3 × 0.2
Space group	<i>P</i> $\bar{1}$	<i>Pbca</i>	<i>P2₁/n</i>
<i>a</i> /Å	11.828(1)	15.750(3)	15.985(2)
<i>b</i> /Å	12.789(1)	28.394(5)	7.419(1)
<i>c</i> /Å	11.766(1)	11.415(1)	14.994(2)
<i>a</i> (°)	101.05(1)		
<i>β</i> (°)	111.04(1)		110.37(1)
<i>γ</i> (°)	97.78(1)		
Unit cell volume/Å ³	1589.3(3)	5105(1)	1667.0(4)
<i>Z</i>	1	8	4
<i>D_c</i> /g cm ⁻³	1.34	1.25	1.38
<i>μ</i> (Cu-Kα)/mm ⁻¹	2.13	1.37	0.85
Collected reflections	4973	4267	2799
Unique reflections	4705	4267	2693
<i>R_{int}</i>	0.014		0.021
Observed reflections, <i>m</i>	4235	2812	2224
Transmission coeff.	0.6121/0.9995	0.7797/0.9998	0.8267/0.9995
No. of variables, <i>n</i>	539	423	299
<i>R^a</i>	0.066	0.071	0.037
<i>R_w^b</i>	0.095	0.089	0.051
GOF ^c	2.974	1.527	1.397
Final residual/e Å ⁻³	-0.13/0.67	-0.46/0.37	-0.20/0.15

^a $R = \sum |F_o| - |F_c| / \sum |F_o|$. ^b $R_w = [\sum w(|F_o| - |F_c|)^2 / \sum w F_o^2]^{1/2}$. ^c $GOF = [\sum w(|F_o| - |F_c|)^2 / (m - n)]^{1/2}$.

2.5)-acetonitrile (1:1) solution. Single crystals of **1** and **3** were grown by slow evaporation from diethyl ether and methanol, respectively. All X-ray data were collected on an Enraf-Nonius CAD4 diffractometer with graphite-monochromated Cu-Kα radiation ($\lambda = 1.5418 \text{ \AA}$).[†] Crystal data and details of the structure determinations are given in Table 3. Unit cell parameters were obtained from least-squares refinement using the setting angles of 25 reflections in the range $20^\circ < \theta < 30^\circ$ for **1** and **2**, and $40^\circ < \theta < 45^\circ$ for **3**. Intensity data were collected at room temperature using the ω - 2θ scan mode to a maximum θ value of 60° . Three standard reflections were monitored every 120 min of exposure time. They showed no significant decay for **1** and **3**. For **2**, a linear decay of 12.8% was observed over the period of data collection, and the data were corrected for the decay. The data were corrected for Lorentz and polarization, but not for absorption. Independent reflections with $F > 3\sigma(F)$ were used in structure solution and refinement. The structures were solved by direct methods using MULTAN 11/82¹⁰ and subsequent Fourier syntheses. All non-hydrogen atoms were refined anisotropically. The positions of hydrogen atoms bonded to nitrogen atoms were located from difference Fourier maps. All other hydrogen atoms except those of disordered carbon atoms and solvent molecules were calculated geometrically. All hydrogen atoms were fixed for **1** and **2**, and refined isotopically for **3**. The structures were refined by full-matrix least-squares using the MOLEN program system,¹¹ and weights were applied in the final cycles of refinement according to the scheme $w = [\sigma(F)^2 + 0.004F + 1]^{-1}$.

The structure of **2** has a centre of inversion with half the molecule consisting of C₂₇H₃₂N₂O₄S·HClO₄·H₂O·CH₃CN in the asymmetric unit. Oxygen atoms of a perchlorate anion were disordered. Two atoms of the acetonitrile molecule were found to be statistically distributed over two positions, and they were located with 0.6 and 0.4 site occupancies, respectively. In the final difference Fourier map four highest peaks (0.47–0.67 e Å⁻³) were located near the perchlorate anion.

[†] Atomic coordinates, thermal parameters, and bond lengths and angles have been deposited at the Cambridge Crystallographic Data Centre (CCDC). See 'Instructions for Authors', *J. Chem. Soc., Perkin Trans. 2*, 1997, Issue 1. Any request to the CCDC for this material should quote the full literature citation and the reference number 188/69.

Three carbon atoms of the piperidine ring of **1** were found to be statistically distributed over two positions; C25–C27 and C25'–C27' were located with 0.7 and 0.3 site occupancies, respectively.

References

- V. Ramamurthy and K. Venkatesan, *Chem. Rev.*, 1987, **87**, 433.
- (a) M. D. Cohen and G. M. J. Schmidt, *J. Chem. Soc.*, 1964, 1996; (b) M. D. Cohen, G. M. J. Schmidt and F. I. Sonntag, *J. Chem. Soc.*, 1964, 2000; (c) G. M. J. Schmidt, *Pure Appl. Chem.*, 1971, **27**, 647.
- (a) S. Ariel, S. Askari, J. R. Scheffer, J. Trotter and L. Walsh, *J. Am. Chem. Soc.*, 1984, **106**, 5726; (b) D. Kanagapushpam, V. Ramamurthy and K. Venkatesan, *Acta Crystallogr., Sect. C*, 1987, **43**, 1128.
- M. D. Cohen, *Angew. Chem., Int. Ed. Engl.*, 1975, **14**, 386.
- A. Gavezzotti, *J. Am. Chem. Soc.*, 1983, **105**, 5220.
- K. Araki, H. Ao, J. Inui and K. Aihara, EP 88 903/1983 (*Chem. Abstr.*, 1984, **100**, 85 591).
- (a) L. J. Nunez-Vergara, C. Sunkel and J. A. Squella, *J. Pharm. Sci.*, 1994, **83**, 502; (b) A. L. Zanocco, L. Diaz, M. Lopez, L. J. Nunez-Vergara and J. A. Squella, *J. Pharm. Sci.*, 1992, **81**, 920; (c) Y. Matsuda, R. Teraoka and I. Sugimoto, *Int. J. Pharm.*, 1989, **54**, 211.
- (a) A. M. Triggie, E. Shefter and D. J. Triggie, *J. Med. Chem.*, 1980, **23**, 1442; (b) R. Fossheim, K. Svarteng, A. Mostad, C. Romming, E. Shefter and D. J. Triggie, *J. Med. Chem.*, 1982, **25**, 126; (c) R. Fossheim, A. Joslyn, A. J. Solo, E. Luchowski, A. Rutledge and D. J. Triggie, *J. Med. Chem.*, 1988, **31**, 300; (d) D. A. Langs, P. D. Strong and D. J. Triggie, *J. Comput.-Aided. Mol. Des.*, 1990, **4**, 215; (e) A. Miyamae, S. Koda and Y. Morimoto, *Chem. Pharm. Bull.*, 1986, **34**, 3071; (f) G. Rovnyak, N. Andersen, J. Gougoutas, A. Hedberg, S. D. Kimball, M. Malley, S. Moreland, M. Porubcan and A. Pudzianowski, *J. Med. Chem.*, 1988, **31**, 936; (g) A. Hempel and M. P. Gupta, *Acta Crystallogr., Sect. B*, 1978, **34**, 3815.
- F. H. Allen, J. E. Davies, J. J. Galloy, O. Johnson, O. Kennard, C. F. Macrae, E. M. Mitchell, G. F. Mitchell, J. M. Smith and D. G. Watson, *J. Chem. Inf. Comput. Sci.*, 1991, **31**, 187.
- P. Main, S. J. Fiske, S. E. Hull, L. Lessinger, G. Germain, J.-P. Declercq and M. M. Woolfson, MULTAN 11/82, *A System of Computer Programs for the Automatic Solution of Crystal Structures from X-ray Diffraction Data*, University of York, England, and Louvain, Belgium, 1982.
- C. K. Fair, MOLEN, *An Interactive Intelligent System for Crystal Structure Analysis*, Enraf-Nonius, Delft, The Netherlands, 1990.

Paper 6/08454K
Received 17th December 1996
Accepted 3rd March 1997